Supporting Information

for

Synthesis and photocatalytic activity of $LaTiO_2N$ using titanium oxide nanosheet/La^{3+} hybrids as a precursor

Xiong Tao[a], Tatsuki Tsugawa[a], Kazuto Hatakeyama[a,b] , Shintaro Ida[a, b, c] *

[a] Graduate School of Science and Technology, Kumamoto University, 2-39-1 Kurokami, Chuo-ku, Kumamoto, 860-8555, Japan.

[b] Institute of Industrial Nanomaterials (IINa), Kumamoto University, 2-39-1 Kurokami, Chuo-ku, Kumamoto, 860-8555, Japan.

[c]Center for Energy Systems Design (CESD), Kyushu University, 744 Motooka, Nishi-ku, Fukuoka 819–0395, Japan

*Corresponding authors at: Institute of Industrial Nanomaterials, Kumamoto University, Kumamoto 860-8555, Japan; orcid.org/0000- 0002-0032-1897;

Email: ida-s@kumamoto-u.ac.jp

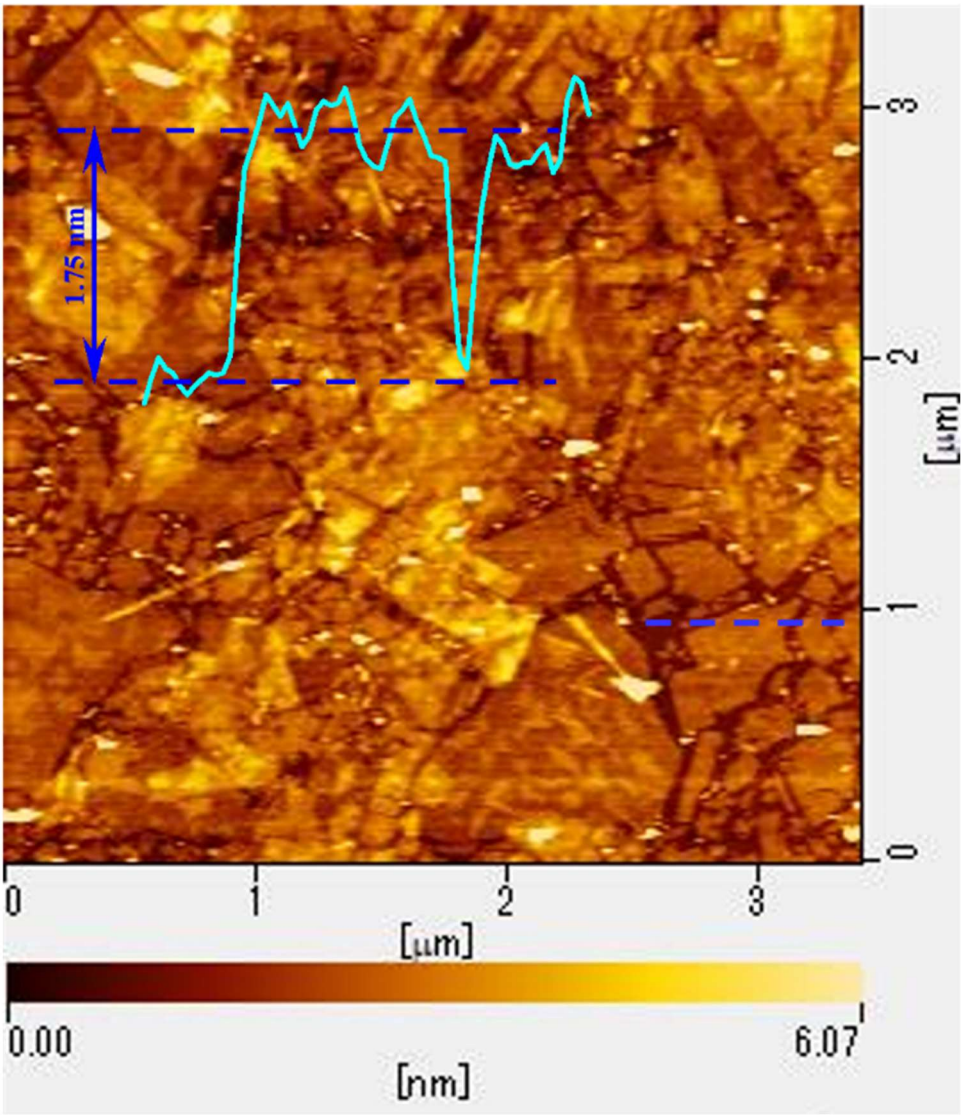

Figure S1. AFM image of exfoliated titanium oxide nanosheet.

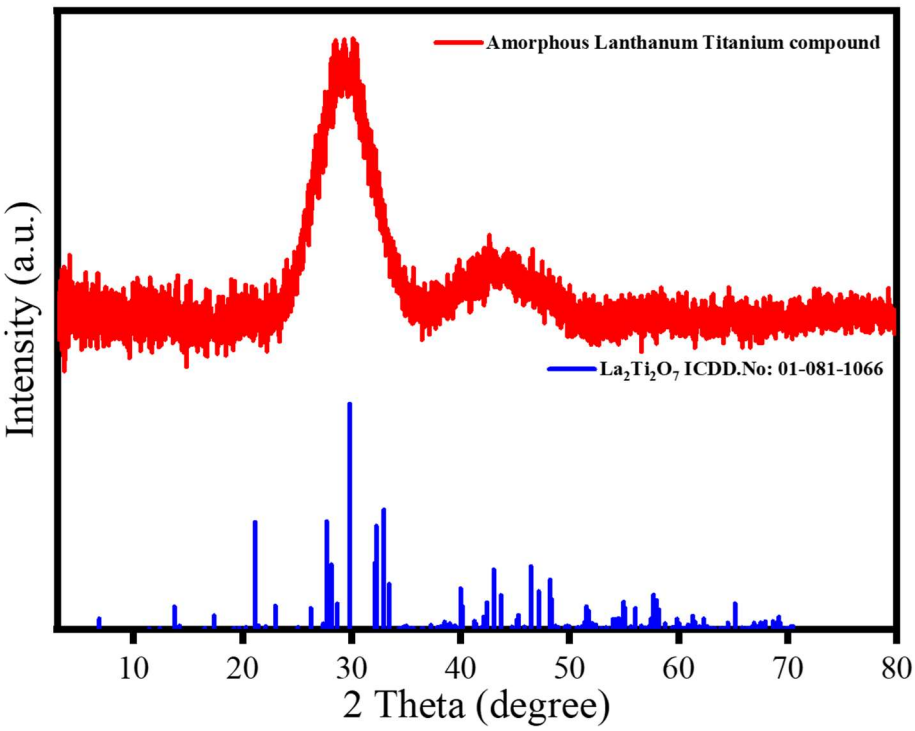

Figure S2. XRD pattern of precursor before the nitride of LTON.

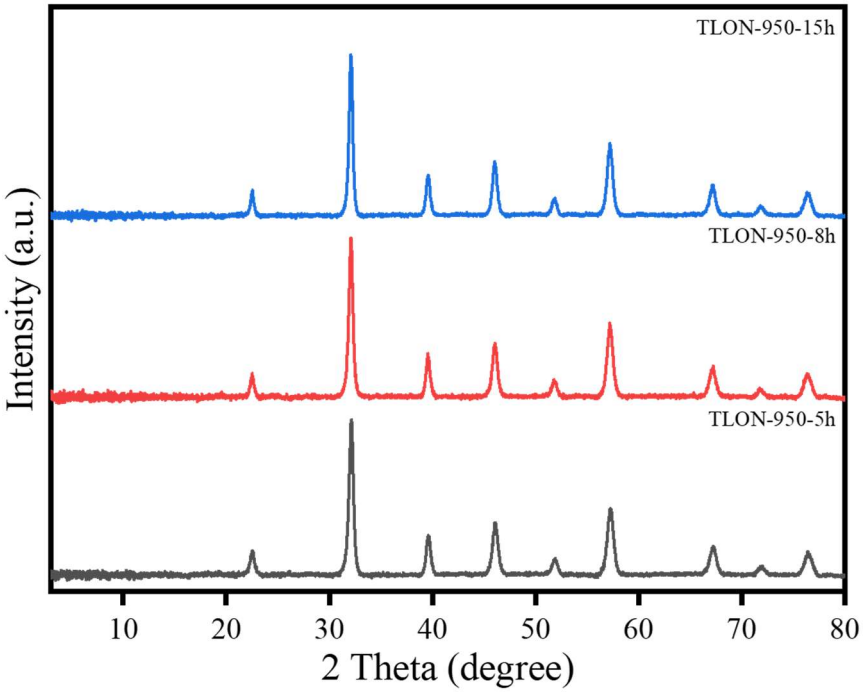

Figure S3. XRD patterns of LTON-950-15h, LTON-950 (LTON-950-8h) and LTON-950-5h.

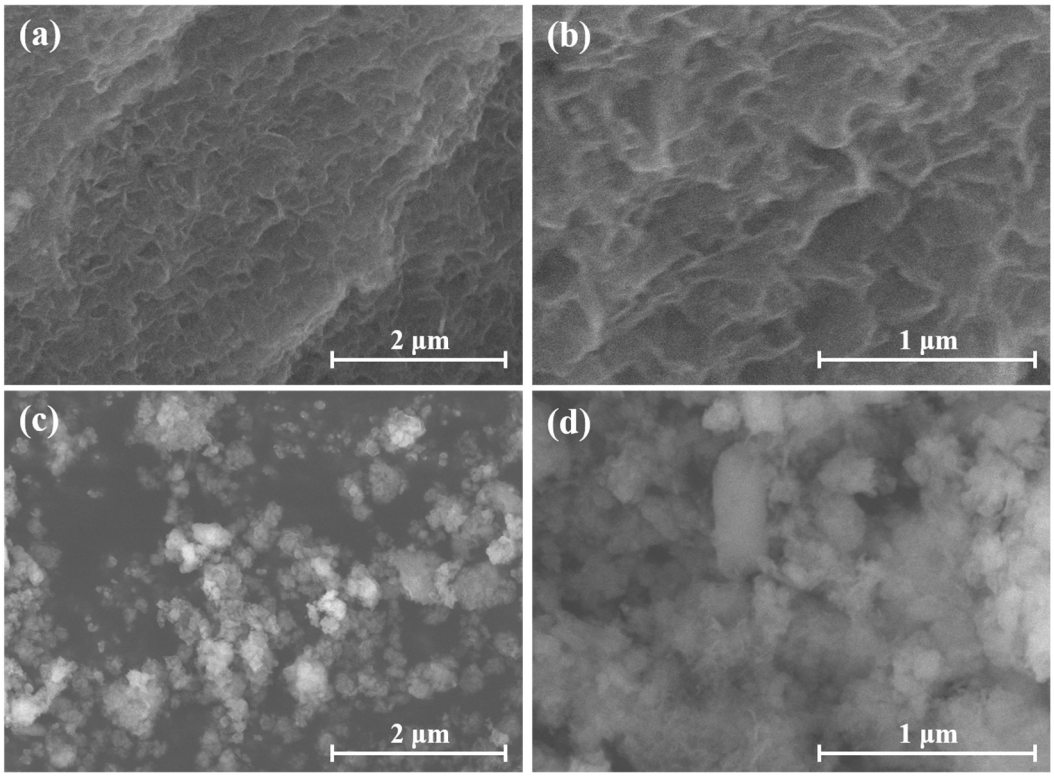

Figure S4. SEM image of the precipitation of titanium oxide nanosheet and La^{3+} ((a) and (b)); The SEM image of amorphous lanthanum titanium compound ((c) and (d)).

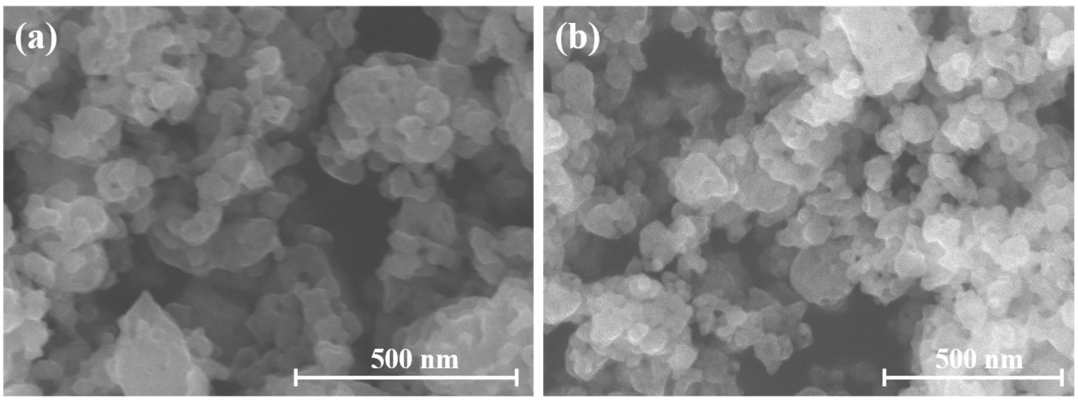

Figure S5. SEM image of LTON-950-5h (a) and LTON-950-15h (b).

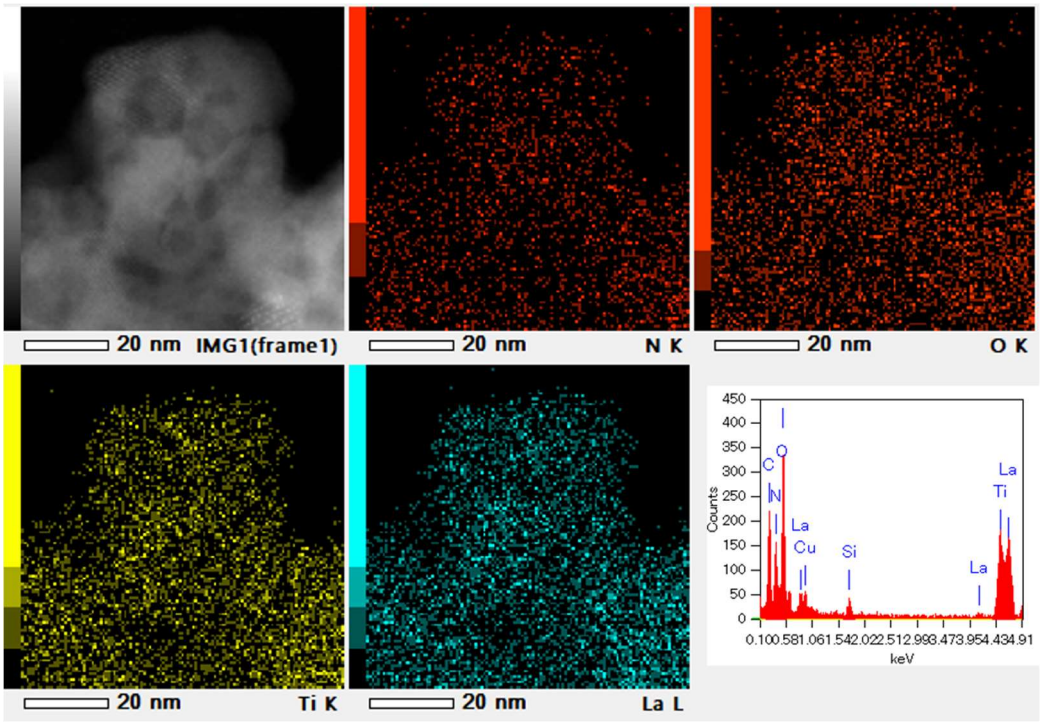

Figure S6. STEM EDS mapping images of LTON-950.

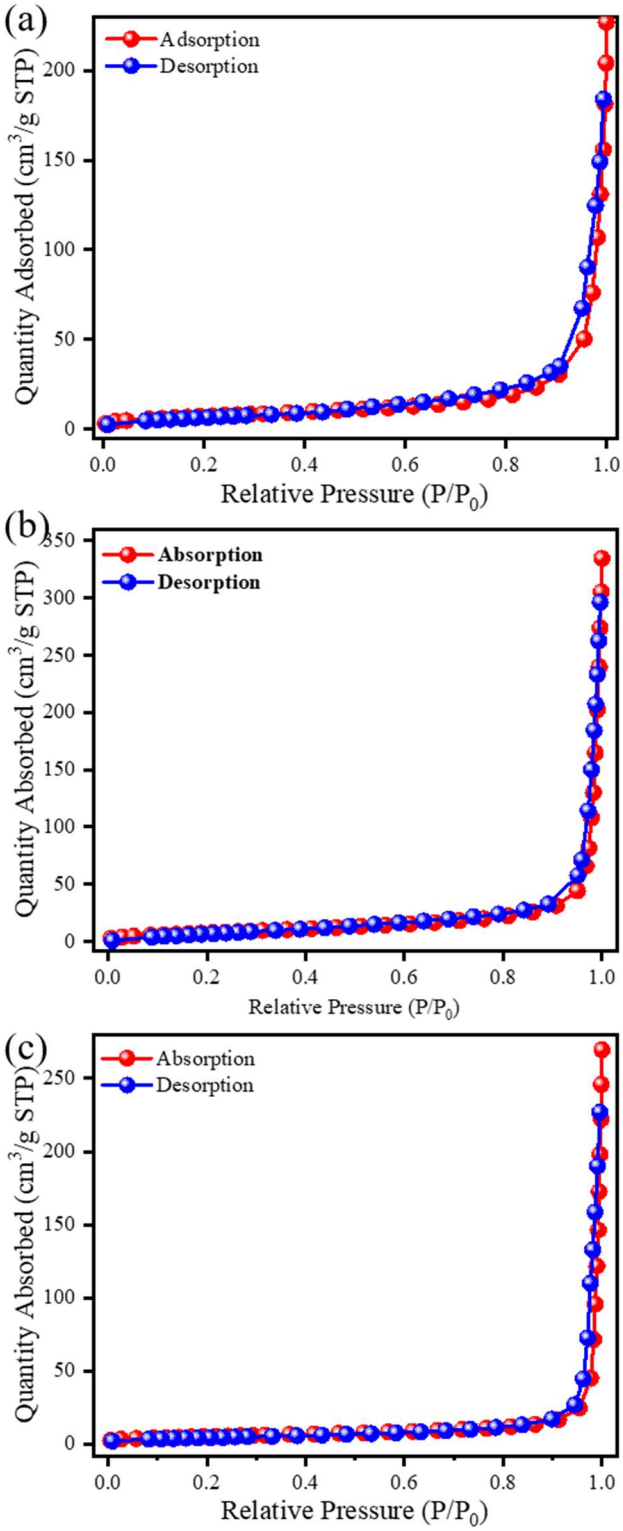

Figure S7. N_2 absorption and desorption isotherm on LTON-900 (a), LTON-950 (b) and LTON-1000 (c).

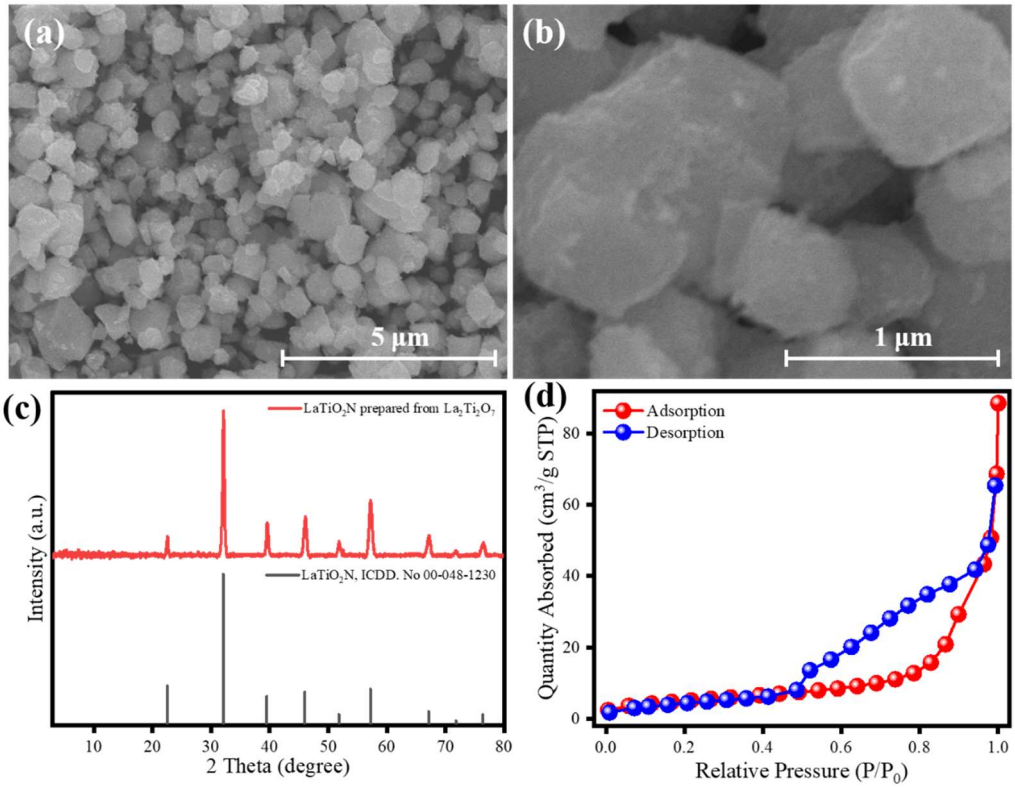

Figure S8. The FE-SEM image ((a) and (b)), XRD and adsorption-desorption isotherm of $LaTiO_2N$ prepared from $La_2Ti_2O_7$.

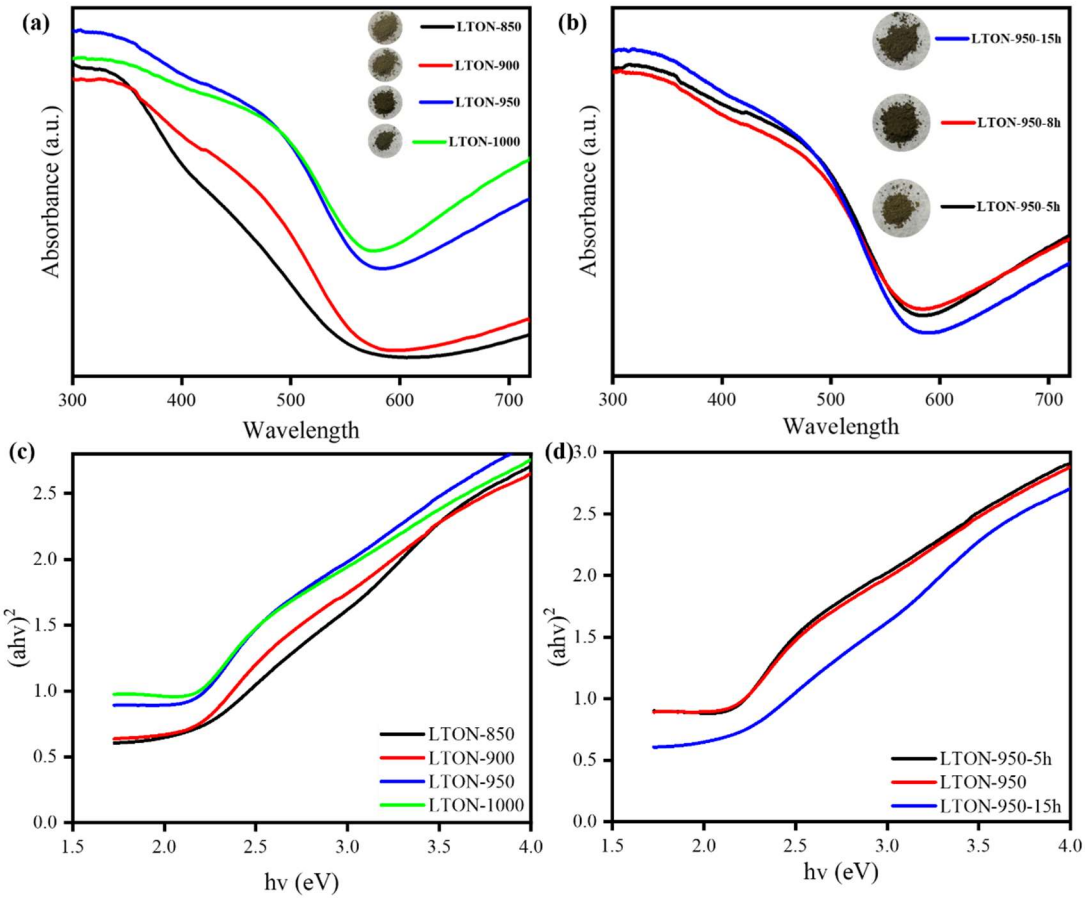

Figure S9. UV–Vis light absorption spectra of synthesized samples ((a) and (b)). Kubelka- Munk transformation of diffuse reflectance data of synthesized samples ((c) and (d)).

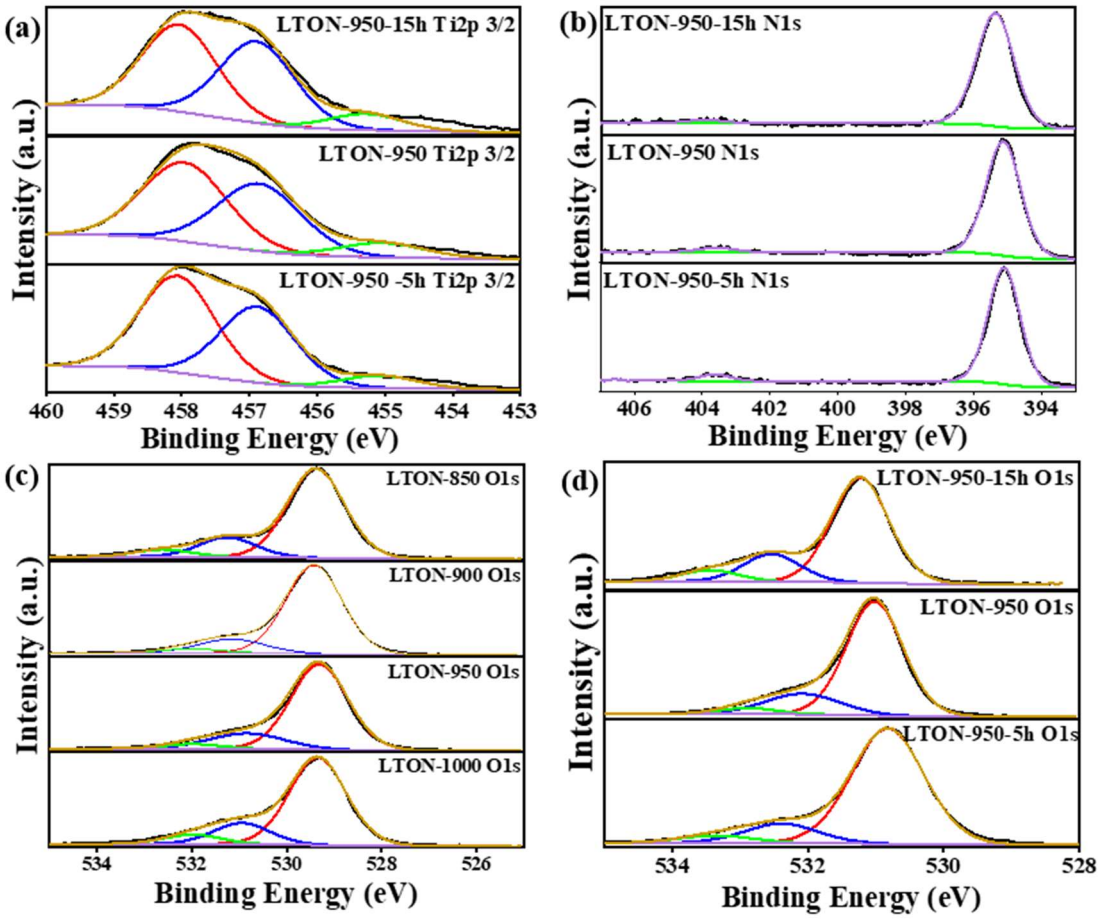

Figure S10. XPS spectra of Ti 2p3/2 (a) and N 1s (b) on LTON-950-5h, LTON-950-8h and LTON-950-15h (a); The high-resolution XPS spectra of O 1s on LTON synthesized at different temperature (c), and different time (d).

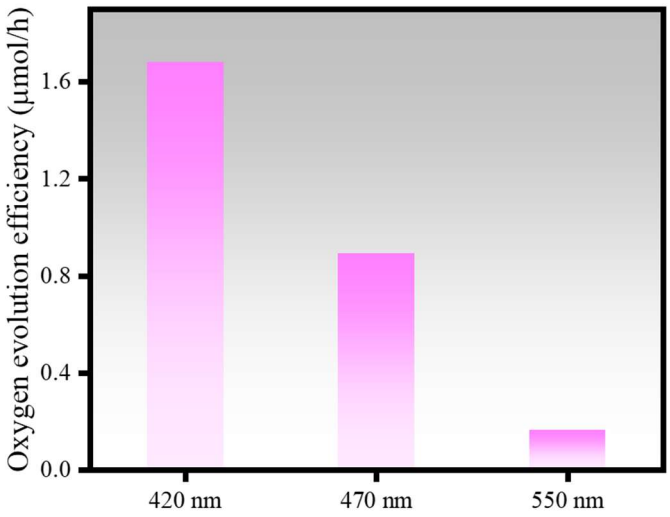

Figure S11. The oxygen evolution efficiency of LTON under light irradiation with different wavelengths.